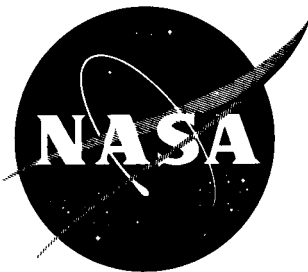


38p.



N63 18663

CODE-1

# TECHNICAL NOTE

## D- 1891

SOME FLIGHT CHARACTERISTICS OF A DEFLECTED  
SLIPSTREAM V/STOL AIRCRAFT

By Howard L. Turner and Fred J. Drinkwater III

Ames Research Center  
Moffett Field, Calif.

NATIONAL AERONAUTICS AND SPACE ADMINISTRATION  
WASHINGTON

July 1963

NATIONAL AERONAUTICS AND SPACE ADMINISTRATION

---

TECHNICAL NOTE D-1891

---

SOME FLIGHT CHARACTERISTICS OF A DEFLECTED  
SLIPSTREAM V/STOL AIRCRAFT

By Howard L. Turner and Fred J. Drinkwater III

SUMMARY

18 663

The Ryan VZ-3RY V/STOL test vehicle was flight tested over the airspeed range from 80 knots to below 6 knots. The deflected slipstream concept proved to be better suited to STOL than VTOL operation. Adverse ground effects prevented operation close to the ground at speeds less than 20 knots and below approximately 15 feet altitude.

Steep glide slopes to landing (up to  $-16^{\circ}$ ) at approximately 40 knots were achieved, but steep, slow, descending flight did not appear feasible. Full-span leading-edge slats markedly increased the descent capability and reduced the minimum level flight speed.

INTRODUCTION

The VZ-3RY deflected slipstream V/STOL aircraft differs from conventional propeller aircraft by the use of a high thrust-to-weight ratio, and oversized full-span flaps deflected through large angles to turn the propeller slipstream flowing over the wing. Changes in power and flap configurations required for flight over the design speed range produce moment variations and wing stall which constitute basic aerodynamic problems in the design of a V/STOL vehicle based on the deflected-slipstream concept. Other problem areas include the provision for adequate controllability of the vehicle over its entire range of operating airspeeds, low propulsive efficiencies, low turning effectiveness, and the effects of operating in close proximity to the ground.

Considerable wind-tunnel work was completed by the NACA on the more basic aerodynamic problems of operating a flapped wing immersed in a propeller slipstream. Results of some of these studies have been published in references 1 to 4. In general, these data indicate that wing stall, at high power and large flap deflections, can limit low-speed flight even though the wing is completely immersed in the propeller slipstream.

To explore some of these problems in flight, the U. S. Army contracted with the Ryan Aeronautical Company in 1957 to develop and build the VZ-3RY "test-bed" with V/STOL capability. The bulk of recent experience with deflected slipstream V/STOL aircraft in the U. S. has been intimately associated with the Ryan VZ-3RY (reported in refs. 5 to 9). It is recognized that certain adverse characteristics are peculiar to the particular test vehicle and would not be general characteristics of the V/STOL concept represented. With this in mind, only data which are felt to be of a general nature are presented in the body of the report. Those characteristics appearing to be peculiar to the Ryan VZ-3RY are presented in the appendix.

In this report, data are presented for the speed range from 0 to 80 knots; however, emphasis has been placed on flight performance data in the STOL flight region above 20 knots. It was previously demonstrated (see ref. 9) that a deflected slipstream V/STOL aircraft can be flown at zero airspeed, out of ground effect, but it was apparent that operation at low airspeeds and low altitudes would, at best, be very marginal because of an adverse ground effect. The limitations of the hovering characteristics of the deflected slipstream vehicle were not deemed to be within the scope of this investigation.

#### NOTATION

$V_i$	indicated airspeed
$W$	gross weight
$S$	wing area with flaps up
$\alpha$	angle of attack
$\gamma$	flight-path angle
$\delta_f$	flap angle
$\delta_t$	horizontal stabilizer incidence for longitudinal trim

#### AIRCRAFT AND CONTROL SYSTEMS

##### Aircraft

The Ryan VZ-3RY deflected slipstream test vehicle, shown in figure 1 with flaps fully deflected and with a leading-edge slat installed, is a single-place, high-wing monoplane powered by a single Lycoming YT-53 free-turbine engine. The power turbine is connected to two counterrotating controllably-pitch propellers through connecting drive shafts. A three-view drawing of the aircraft is shown in figure 2. Pertinent dimensions are given in table I.

Tests were made with and without full-span leading-edge slats on the wing. A diagram of the slat installation is given in figure 3. Photographs of the slat, as flight tested, are shown in figure 4.

### Flight Control Systems

The Ryan VZ-3RY test vehicle was equipped with dual modes of control about pitch, roll, yaw, and thrust axes to permit flight at airspeeds above and below speeds where conventional controls are effective. These flight control systems are described in the paragraphs below.

Longitudinal control systems.- The longitudinal control systems include a conventional control stick mechanically connected by cables to a conventional elevator incorporating a geared tab. A thrust diverter, mechanically connected to the elevator and mounted on the aft end of the exhaust-gas tailpipe, utilizes residual thrust from the engine to provide the control moment at airspeeds for which the conventional elevator is ineffective. The control moment produced by residual thrust varied as a direct function of output horsepower. During flight both aerodynamic and reaction control systems are operating. Longitudinal trim is provided by an all-movable horizontal stabilizer actuated by an electric motor; the incidence range is  $13^{\circ}$  to  $23^{\circ}$  (with respect to the fuselage reference line). A conventional thumb-operated trim switch is provided on top of the control stick.

A total of  $32.3^{\circ}$  of elevator was available to the pilot for a total of 14 inches of stick travel.

Lateral control systems.- The lateral control systems installed in the Ryan VZ-3RY include slot-lip spoilers for aerodynamic control and differential propeller pitch for low-speed lateral control. Differential propeller pitch was automatically varied with the deflection of the flaps, from  $0^{\circ}$  blade angle at  $0^{\circ}$  of flap to  $\pm 1.5^{\circ}$  blade angle at  $65^{\circ}$  of flap (for full stick travel of  $\pm 7\frac{1}{2}$  inches). Considerable difficulty was encountered with "snatching" of the slot-lip spoilers when the flaps were retracted. This phenomenon was traced to the configuration established between the upper surface of the flap and the lower surface of the spoiler (see fig. 2). Perforating the spoiler with  $\frac{1}{2}$ -inch-diameter holes eliminated the snatching without reducing the spoiler effectiveness.

Fixed, bendable tabs were added to the outboard trailing edges of both the spoilers and the lower flap surfaces. Breakout forces for the latter controls were less than 16 ounces.

The pitch change mechanism of the propeller blades was dependent on hydraulic pressure (500 psi) to drive the blades to low pitch and a combination of counterweight forces and aerodynamic forces on the blades to drive the propeller toward high pitch. Difficulties were encountered initially in making abrupt blade angle changes due to lags resulting from differences in internal friction of the propellers. After the propellers were reworked to produce blade angle changes at rates up to  $16^{\circ}$  per second with differential lags of less than 0.10 second they provided satisfactory control response characteristics.



Directional control systems.- The directional control systems of the Ryan VZ-3RY consisted of a conventional rudder for high-speed flight and a series of shutters attached to the thrust diverter for control at low airspeeds. The rudder and thrust diverter were mechanically connected together and operated at all times during flight.

Thrust control.- Thrust control was provided by a throttle, which controlled fuel flow to the gas generator section of the free-turbine engine, and also by a collective pitch lever which controlled the propeller blade angles. When the latter control was used, fuel flow for the engine was regulated by the governor of the power turbine. Both the throttle and the collective pitch control were mounted side by side along the forward, left side of the cockpit, with the throttle mounted outboard of the collective pitch control.

It was determined that height control of the VZ-3RY was more readily accomplished by collective pitch changes of the propeller blade angles than by thrust changes with the throttle because of the increased response allowable with the former system. This feature was not extensively used in these flight tests, however, because the propeller blade angle could not be set below that required for power-off flight and this minimum blade angle resulted in excessive horsepower output at governed RPM.

## TESTS, RESULTS, AND DISCUSSION

### Handling Qualities

While it can be argued that certain handling qualities of the deflected slipstream test vehicle are peculiar to the Ryan VZ-3RY, control power and damping, lateral-directional coupling, and stalling characteristics are of a general nature and will be discussed in this section of the report. Other characteristics of the VZ-3RY, such as the longitudinal stability and trim characteristics, lateral-directional stability characteristics, and the flight operating boundaries, are reported and discussed in the appendix.

Control power and damping.- The maximum longitudinal control powers available, utilizing combined aerodynamic and reaction controls are given below for three airspeeds. The corresponding damping values and pilot opinion ratings (based on the scale of ref. 10) are also included.

Airspeed, knots	Flap angle, deg	Control power, radians/sec <sup>2</sup>	Rate damping, per sec	Pilot opinion rating
20	65	1.00	-0.945	3
35	40	1.63	-1.76	3
60	20	2.00	-2.89	3

It should be noted that pilot opinion ratings shown in the table above reflect the pilot's opinion of the longitudinal response and not the over-all longitudinal controllability of the aircraft. Although the pilots found that

the control powers available were adequate, the neutral or negative stability characteristics (see appendix) reduced the pilot opinion rating of the longitudinal controllability to 4-1/2, an unsatisfactory value.

The maximum lateral control powers available with combined spoiler and differential propeller pitch are given below for three airspeeds. The corresponding damping and pilot opinion ratings are also included.

Airspeed, knots	Flap angle, deg	Control power, radians/sec <sup>2</sup>	Rate damping, per sec	Pilot opinion rating
20	65	4.5	-0.68	2
35	40	2.6	-0.90	2
60	20	1.35	---	4

Again, the pilot opinion ratings shown above reflect the pilot's opinion of the lateral response and not the lateral controllability of the aircraft. A lateral-directional coupling problem reduced the pilot opinion rating of controllability to 6.5, an unacceptable value. This problem will be discussed in the next section of the report.

Measurements of yaw control power and damping are not presented since full directional control (rudder plus thrust diverter) did not produce an appreciable yawing acceleration over the speed range tested. During flight at 20 knots in still air the directional stability was so low that the small yawing moments produced by the spoilers and differential propeller pitch resulted in sideslip excursions as much as  $\pm 10^\circ$ . Yaw damping appeared to be very high. The pilot rated the directional control as 8, an unacceptable value.

Lateral-directional coupling.- A time history of an aileron step (rudder fixed) is shown in figure 5. These data were obtained at 20 knots with  $65^\circ$  of flap. It will be noted that large values of sideslip develop before any appreciable yawing velocity develops. As a result, unless rudder is used, the aircraft will turn only after an appreciable time delay. This unsatisfactory characteristic occurs during roll maneuvers at low speeds where the directional stability of the vehicle is apparently poor. A similar roll-sideslip coupling problem was encountered with the BLC equipped NC-130B in low-speed flight (ref. 11).

Stall and minimum speed characteristics.- The stalling characteristics consisted of small excursions in pitch and roll with moderate buffeting for flap deflections less than  $40^\circ$ . For higher flap deflections the stall was more gentle with a mild loss in lift. No serious buffeting or roll off was encountered.

The minimum airspeed to which the aircraft could be flown in level flight (at power for level flight) without the leading-edge slats (ref. 5) was 24 knots. Slats made possible a large reduction in minimum level flight airspeed and a corresponding large increase in angle-of-attack capability. Data showing the increased angle-of-attack range available are given in figure 6.

With only aerodynamic longitudinal and directional control the aircraft was flown with 50° of flap to a minimum airspeed of 35 knots (without slats). The aircraft did not stall, but control power about the longitudinal and directional axes by aerodynamic means alone was completely unacceptable and limited the minimum speed to which the aircraft could be flown.

### Performance Characteristics

Flight performance characteristics are shown in figure 7. The upper boundary was determined at maximum power. The lower boundary from 66 to 38 knots was obtained at flight idle power, with an increase in flap deflection from 0° at 66 knots to 40° at 38 knots. This latter point represents the minimum airspeed at which lateral control is acceptable with flight idle power.<sup>1</sup> Further decreases in airspeed are possible only by increasing power and flap deflection; however, there is a marked decrease in descent capability under these conditions. Without wing slats, the minimum level flight speed obtainable was 24 knots. With wing slats, zero airspeed could be obtained but with very low descent rate capability. (It should be noted that the accuracy of airspeed measurements below 6 knots was doubtful because the flow field around the aircraft limited the accuracy of the balanced thermocouple hot wire anemometer used to measure airspeed below 10 knots.)

It is apparent from figure 7 that increases in power to permit flight at lower speeds compromised descent capability. No reasonable modifications or operating techniques were found which would permit steep descents at low speeds. The thrust vector could not be oriented in a direction such as to produce a braking force and still provide reduced stall speeds. Wing stall is induced by increasing descent rate. Positioning the aircraft in a minimum speed nose-high attitude and establishing high rates of sink required further increases in both airspeed and descent rate to arrest the sink. This was not considered a desirable maneuver. The inability to utilize power to obtain low-speed steep descents was also a characteristic found in both the C-130 and the C-134 BLC research aircrafts (refs. 11 and 12).

At very low airspeeds, steep descents in a nose-high attitude were limited by unsteady flight associated with wing stall. At airspeeds as low as 10 knots, where it is usually assumed that the influence of free-stream dynamic pressure can be neglected, the effect of angle of attack was pronounced and wing stall could still be induced in level flight by small increases in descent rate or by reduction in power. This was true even though the physical geometry of the slipstream with respect to the wing was apparently unchanged and the whole span was immersed in the propeller slipstream.

The foregoing slow speed characteristics are for operation out of ground effect. The effects of the proximity to the ground are treated in another section of this report.

---

<sup>1</sup>Flight idle power at 40 knots is approximately 100 horsepower.

## Short Take-Off and Landing Characteristics

Short take-off characteristics.- The short take-off characteristics are shown in figure 8 and include the distance from start of ground run to the point where the aircraft became airborne and from start to clearance over a 50-foot obstacle as functions of flap deflection. All take offs were accomplished with full power. It should be noted that the VZ-3 brake system made it impossible to hold the aircraft with more than 100 horsepower; hence, take-off distances are lengthened somewhat. The throttle was opened fully prior to brake release but 50 percent of the take-off time for the minimum distance take-offs occurred while the engine was accelerating up to full power.

The data of figure 8 were obtained photographically with a Fairchild flight analyzer. A typical short take-off record is shown in figure 9. The performance data have not been corrected for wind. The majority of runs were made in calm air and in no case was the wind velocity greater than 10 knots. A representative time history of a minimum distance take-off, obtained from airborne data recording in the test vehicle, is shown in figure 10. Minimum distance take-offs were accomplished at longitudinal accelerations of 0.5 g and climbouts were accomplished at climb flight-path angles averaging  $25^{\circ}$ . The fuselage attitudes in climbout did not exceed  $15^{\circ}$  nose up. Flap retraction was initiated shortly after the aircraft became airborne. Due to the abrupt nature of the take-off maneuver (4 to 6 sec) the pilot had to be careful to avoid overrotation.

The data of figure 8 show a decrease in take-off distance with an increase in flap deflections up to  $40^{\circ}$  or  $50^{\circ}$ . Further increases in flap deflection lengthened the take-off. It was noted that at flap deflections above  $50^{\circ}$  the recirculation of propeller slipstream and the increased drag due to the extended flaps caused an increase in take-off distance. At  $40^{\circ}$  of flap, take-offs were accomplished in as little as four seconds with as little as 38 feet of ground run and climb angles up to  $33^{\circ}$ . The data of figure 8 represent average values. It is also noted that the wing leading-edge slats improved take-off performance particularly at zero flap setting. At the minimum distances, the time and distance gains due to slats were small. It was felt that the low-wing loading of 23 lb/ft<sup>2</sup> and high power loading of 0.25 hp/lb contributed markedly to the short take-off characteristics.

Short landing characteristics.- The short landing characteristics are shown in figure 11 as functions of flap deflection. These data are for conditions of slats off and slats on, and include touchdowns both with and without flares. Landing roll is not included because the aircraft braking system was not representative of a production airplane.

As would be expected, a decrease in landing speed and distance was obtained up to flap deflections of approximately  $40^{\circ}$ . Further decreases in landing speed by the use of power and flap resulted in increased distance to touchdown because of a flatter approach, particularly without slats. Ground effect problems were encountered at the higher flap deflections when airspeed was reduced to less than 20 knots. The minimum distance to touchdown shown was obtained at  $-16^{\circ}$  glide slope (slats on) and at an approach speed of about 40 knots. The touchdown

airspeed after flare averaged 25 knots. It was considered that this represented the maximum glide slope and the minimum airspeed for short landings while providing an adequate margin from the stall and sufficient lateral and longitudinal control. This point is noted on the performance curves shown in figure 7.

In figure 12 rate of descent is plotted against airspeed for various flap deflections for both the slat-on and slat-off configurations.<sup>2</sup> Maintenance of good flow over the wing was of paramount importance in attaining steep descent in the final approach. Although approach angles to touchdown up to  $-16^{\circ}$  were used, it was felt that approach angles from  $-10^{\circ}$  to  $-15^{\circ}$  represent more realistic values. Steeper approaches produced difficulties in judging the point of flare. In cases where no flare was utilized and the aircraft was flown into the ground, the landing distance was reduced (see fig. 11). High sink-rate operation would compromise the aircraft's over-all performance by calling for a heavy landing gear.

### Representative STOL Operating Profile

In view of the STOL performance experience with the deflected slipstream test vehicle and with consideration to the operating limitations of such a concept, a mission operating profile is illustrated. A diagram of this profile is shown in figure 13. With reference to this figure, points A to B would be an acceleration to take-off speed at 0.5 to 1.0 g; points B to C, climbout at a maximum of  $25^{\circ}$  to cruise altitude; points C to D, cruise; points D to E, descent at flight idle at a maximum glide slope of  $-25^{\circ}$ ; points E to F, level flight deceleration to approach speed made at obstacle height (plus clearance height); points F to G, final approach at a glide slope of  $-10^{\circ}$  to  $-15^{\circ}$  to touchdown; points G to H, deceleration to full stop at 0.5 to 1.0 g. Climbout and descent could be made in a tight spiral if tactical conditions dictated this type of maneuver. The minimum time and minimum fuel descent from cruise is accomplished at the steepest angle consistent with airspeed limitations D to E. The minimum time and minimum fuel deceleration to the approach speed is accomplished at minimum power and in level flight (or the shallowest possible descent angle E to F). Vertical descent to touchdown do not appear to be technically or operationally useful with the deflected slipstream concept because of the difficulty in obtaining satisfactory height control and because of the adverse, self-generated ground effects discussed in the next section.

### Ground Effects

Operation of the test vehicle was severely limited at airspeeds less than 20 knots when the center line of the propeller was within 1.5 propeller diameters of the ground (approximately 15 feet) due to an adverse, self-generated ground effect. The speed and altitude limitations are probably functions of the velocity of the deflected slipstream and the mass flow through the propellers. In the

---

<sup>2</sup>No significant difference was noted between the airspeeds selected by the pilot for approaches with slats off or slats on.

case of the VZ-3RY, a pictorial examination of the ground effect was made to determine the nature of the flow. Examples are shown in figure 14. In figures 14(a) and (b) the aircraft is flying 1.8 propeller diameters above the ground, out of ground effect, at 24 and 8 knots, respectively. In figure 14(c), the aircraft at 8 knots has entered into ground effect.

To obtain these photographs the runway was dusted with Ansul fire extinguisher powder and the dusted area was flown over at a constant altitude and airspeed.

In general, these photos show the flow pattern of the recirculated air. In figure 14(a), the velocity of the aircraft exceeds the velocity of the air recirculated by the deflected flaps, and the disturbed area, shown by the dust cloud, proceeds somewhat ahead of the flap trailing edge but remains behind the propeller disc. At airspeeds in excess of 20 knots, it was found that the aircraft could operate as close to the ground as possible while still remaining airborne and no adverse ground effect was encountered. In figure 14(b), the velocity of the aircraft is less than the velocity of the recirculated air and the disturbed area shown by the dust cloud proceeds ahead of the propeller disc. However, the aircraft has sufficient height to remain above the recirculated air and hence is not affected by it. In figure 14(c), the aircraft entered into ground effect and lost height before reaching the dusted area. However, the series of pictures show the recirculated air passing through the propeller disc.

The mechanism of the ground effect appears to be that the deflected slipstream is recirculated through the propeller disc as turbulent air, producing, in part, a loss in propeller efficiency, hence, a loss in slipstream velocity and a reduction in turning effectiveness. A loss in lift results from the lowered slipstream velocity and the aircraft sinks rapidly into the ground. It was not possible to check the descent with application of power. A loud slapping noise from the propellers accompanies this loss in lift. The aircraft did not exhibit any tendency to pitch abruptly when entering into ground effect. However, under cross-wind conditions, asymmetric losses in lift were experienced, resulting in abrupt sideslip or abrupt banking of the aircraft just prior to ground contact.

A similar adverse ground effect was noted in wind-tunnel studies of an aircraft with a similar wing loading as reported in reference 13.

#### CONCLUDING REMARKS

Flight tests with the Ryan VZ-3RY V/STOL deflected-slipstream test vehicle have indicated that the concept has some outstanding advantages as a STOL aircraft where very short take-off and landing characteristics are desired. An adverse ground effect, brought about by the recirculation of the propeller slipstream, severely restricted operation at very low airspeeds.

Steep glide slopes (up to  $-16^{\circ}$  at 40 knots) at low horsepower and level flight at very low airspeeds (as low as 6 knots) at high horsepower were readily achieved. However, no operating technique or change in aerodynamic characteristics was found that would permit steep descents at low airspeeds.

It was found that even though the wing was completely immersed in the slipstream of the propeller, unsteady flow over the wing at very low airspeeds resulted in poor flight-path control. Adding full-span leading-edge slats markedly increased the descent capability and resulted in a large decrease in level flight airspeeds.

It was found necessary to augment the aerodynamic controls to fly the vehicle at speeds less than 35 knots.

Ames Research Center

National Aeronautics and Space Administration

Moffett Field, Calif., April 12, 1963

## APPENDIX

### FLIGHT CHARACTERISTICS OF THE RYAN VZ-3RY

#### STABILITY AND CONTROL CHARACTERISTICS

##### Static Longitudinal Stability

The static longitudinal stability characteristics of the Ryan VZ-3RY at the maximum gross weight and the corresponding center-of-gravity position shown in table I are presented in figure 15. The aircraft exhibited neutral or negative stability throughout most of its flight range, particularly with flaps down. Longitudinal control at low horsepower in landing approaches and during the flare was considered satisfactory. The effect of the installation of the wing slats was to decrease the airspeed at which the aircraft could be flown for each flap and power setting and hence to make the negative stability more apparent.

##### Longitudinal Trim

The longitudinal trim characteristics of the aircraft without slats have been previously reported in reference 5; hence, only the effects of the slats on the angle of attack required for level flight are repeated here. These data were shown in figure 6. It will be noted that the leading-edge slats allowed the aircraft to be flown to a considerably higher angle of attack and, hence, lower airspeed.

The effects of horizontal-tail incidence, flaps, and power on the longitudinal trim are shown in figure 16. It will be noted that the effects of flaps and power on trim are small, probably because the nose-down pitching moments produced by the deflection of the flaps are offset by the nose-up pitching moments produced by the changes in power that accompany the flap changes. This would not be the case if the center line of the propeller passed above the airplane center of gravity as it normally would on a high wing monoplane with the nacelles mounted close to the wing reference line.

##### Steady Sideslip Characteristics

The effects of steady sideslip on bank angle required for trim and on the rudder required for trim are shown in figure 17. These data showed a marked change in sideslip attainable at the different powers associated with the various flap deflections noted. The thrust diverter was realigned to remove the yawing moment due to power but since the bank angle required to maintain a given



sideslip was small and unaffected by this alinement these data were not retaken. However, it is evident from these data that the directional control of any airspeed or flap deflection was inadequate.

#### FLIGHT OPERATING BOUNDARIES

The minimum and maximum airspeed-flap deflection boundaries over which the deflected slipstream test vehicle was operated are shown in figure 18. The maximum airspeeds allowable for each flap deflection were dictated by the structural strength of the wing flaps. The minimum airspeed boundaries at flight idle power were dictated by wing stall up to flap deflections of  $40^{\circ}$  and by lack of lateral control at flap deflections between  $40^{\circ}$  and  $65^{\circ}$ . The minimum airspeeds obtainable at power for level flight were determined by the airspeed at which level flight could not be maintained. The increase in performance with the wing leading-edge slats installed is apparent. This is primarily due to the increased angle of attack to which the airplane can be flown with the slats on.

## REFERENCES

1. Kuhn, Richard E., and Hayes, William C., Jr.: Wind-Tunnel Investigation of Effect of Propeller Slipstreams on Aerodynamic Characteristics of a Wing Equipped With a 50-Percent-Chord Sliding Flap and a 30-Percent-Chord Slotted Flap. NACA TN 3918, 1957.
2. Kuhn, Richard E., and Draper, John W.: Investigation of Effectiveness of Large-Chord Slotted Flaps in Deflecting Propeller Slipstreams Downward for Vertical Take-Off and Low-Speed Flight. NACA TN 3364, 1955.
3. Kuhn, Richard E., and Draper, John W.: An Investigation of a Wing-Propeller Configuration Employing Large-Chord Plain Flaps and Large-Diameter Propellers for Low-Speed Flight and Vertical Take-Off. NACA TN 3307, 1954.
4. Kuhn, Richard E.: Investigation of Effectiveness of a Wing Equipped With a 50-Percent-Chord Sliding Flap, a 30-Percent-Chord Slotted Flap, and a 30-Percent-Chord Slat in Deflecting Propeller Slipstreams Downward for Vertical Take-Off. NACA TN 3919, 1957.
5. Turner, Howard L., and Drinkwater, Fred J., III: Longitudinal Trim Characteristics of a Deflected Slipstream V/STOL Aircraft During Level Flight at Transition Flight Speeds. NASA TN D-1430, 1962.
6. Parks, W. C., and Davis, W. B.: Stability and Control Investigations of the Ryan Model 92 Deflected Slipstream Airplane Based on Full-Scale Wind-Tunnel Tests. Ryan Aeronautical Co. Rep. 9254-1, July 1959.
7. James, Harry A., Wingrove, Rodney C., Holzhauser, Curt A., and Drinkwater, Fred J., III: Wind-Tunnel and Piloted Flight Simulator Investigation of a Deflected-Slipstream VTOL Airplane, the Ryan VZ-3RY. NASA TN D-89, 1959.
8. Shear, H. J., Jr.: Flight Simulation of the Ryan Model 92 Deflected Slipstream Airplane. Ryan Aeronautical Co. Rep. 9269-4, May 1959.
9. Tuttle, Don T.: Final Flight Test Report, VZ-3RY (Ryan Model 92) Airplane. Ryan Aeronautical Co. Rep. 9269-2, March 1960.
10. Cooper, George E.: Understanding and Interpreting Pilot Opinion. Aero. Eng. Rev., vol. 16, no. 3, March 1957, pp. 47-51, 56.
11. Quigley, Hervey C., and Innis, Robert C.: Handling Qualities and Operational Problems of a Large Four-Propeller STOL Transport Airplane. NASA TN D-1647, 1963.

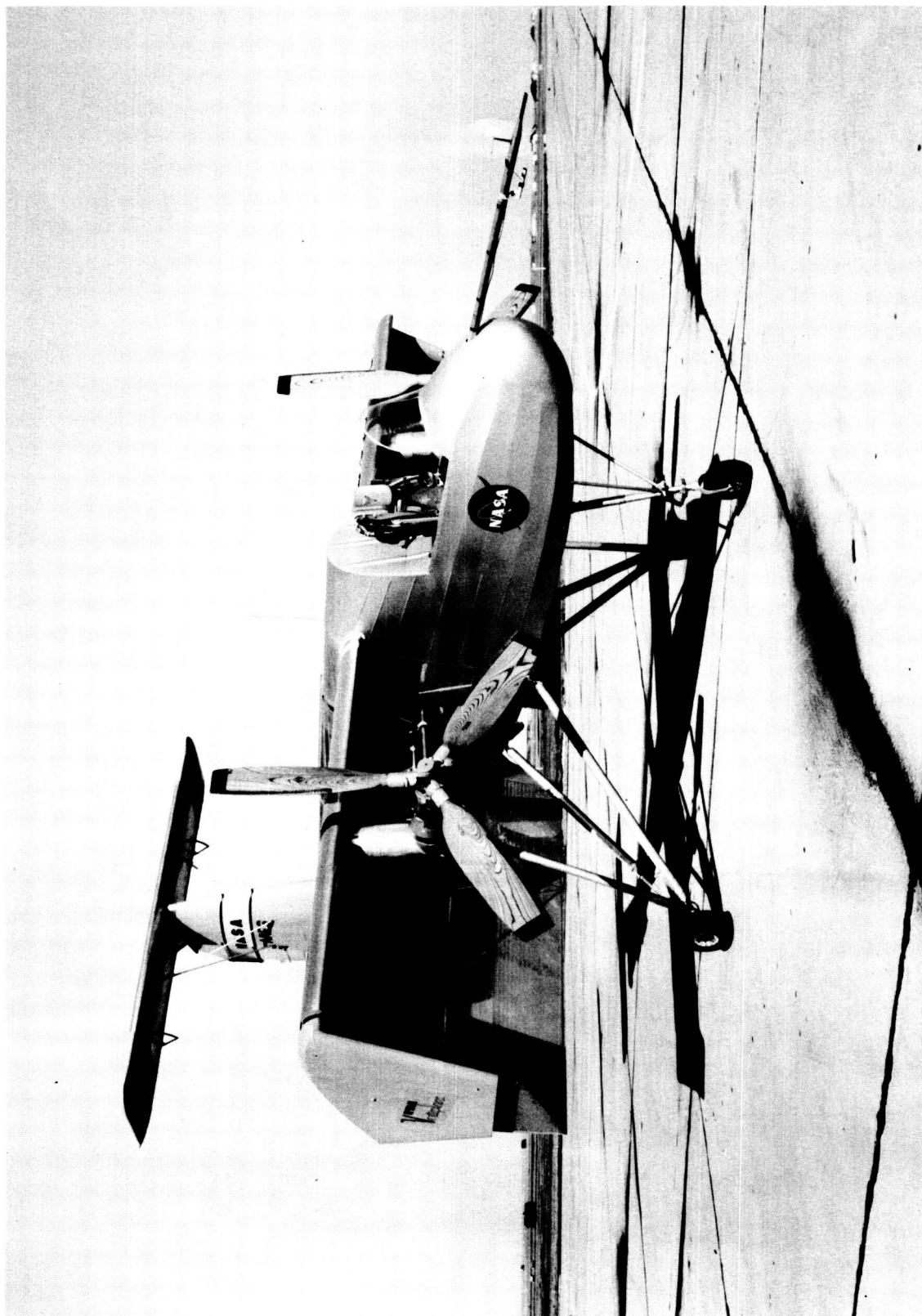
12. Innis, Robert C., and Quigley, Hervey C.: A Flight Examination of Operating Problems of V/STOL Aircraft in STOL-Type Landing and Approach. NASA TN D-862, 1961.
13. Kuhn, Richard E., and Hayes, William C., Jr.: Wind Tunnel Investigation of Longitudinal Aerodynamic Characteristics of Three Propeller-Driven VTOL Configurations in the Transition Speed Range, Including Effects of Ground Proximity. NASA TN D-55, 1960.

TABLE I.- GEOMETRIC DATA, RYAN VZ-3RY

Wing	
Area (flaps up) sq ft	125
Span, ft	23.4
Aspect ratio	4.4
Taper ratio	1.0
Mean aerodynamic chord, ft	5.33
Incidence (relative to fuselage reference line), deg	22
Airfoil	NACA 4418
Flap	
Area (4 flaps), sq ft	126.8
Span (each flap), ft	10.0
Chord, ft	
Upper flap	3.29
Lower flap	3.05
Horizontal tail	
Area, sq ft	64.4
Span, ft	15.4
Aspect ratio	3.7
Taper ratio	1.0
Mean aerodynamic chord, ft	4.18
Elevator area aft of hinge line, sq ft	11.86
Tab area aft of hinge line, sq ft	2.56
Tab gear ratio, deg tab/deg elevator	1.43:1
Tail length (wing $\bar{c}/4$ to horiz. tail $\bar{c}/4$ ), ft	13.76
Incidence change available for trim (incidence reference line inclined $13^\circ$ nose up with respect to fuselage reference line), deg	10
Vertical tail	
Area, sq ft	21.2
Rudder area aft of hinge line, sq ft	4.1
Span, ft	4.7
Fuselage	
Length (including thrust diverter), ft	30.00
Height (max), ft	5.15
Width (max), ft	2.5
Cockpit	open
Ejection seat (rocket-catapult with zero-zero capability)	North American LW-1A
Ejection seat weight (including parachute and catapult), lb	71.5
Engine	
Rated horsepower	Lycoming YT-53 725

Propeller - Hartzell, 3-blade, wood, Model HC-93Z20-1C		
Diameter, ft . . . . .		9.17
Thrust axis relative to fuselage reference line, deg . . . . .		13
Thrust axis toe-out, deg . . . . .		1.5
Thrust axis inclination relative to wing chord line, deg . . . . .		-9.0
Weight and balance		
Maximum gross weight, lb . . . . .		2925
Center of gravity (at maximum gross weight), inches aft of leading- edge mean aerodynamic chord . . . . .		21.10
Vertical center of gravity (below fuselage reference line, in.) . .		6.61

Note: Thrust axis passes 1.87 inches below center of gravity at longitudinal center-of-gravity position.



A-30017

Figure 1.- The Ryan VZ-3RY deflected-slipstream test vehicle shown with leading-edge slat installed and with fully extended flaps.

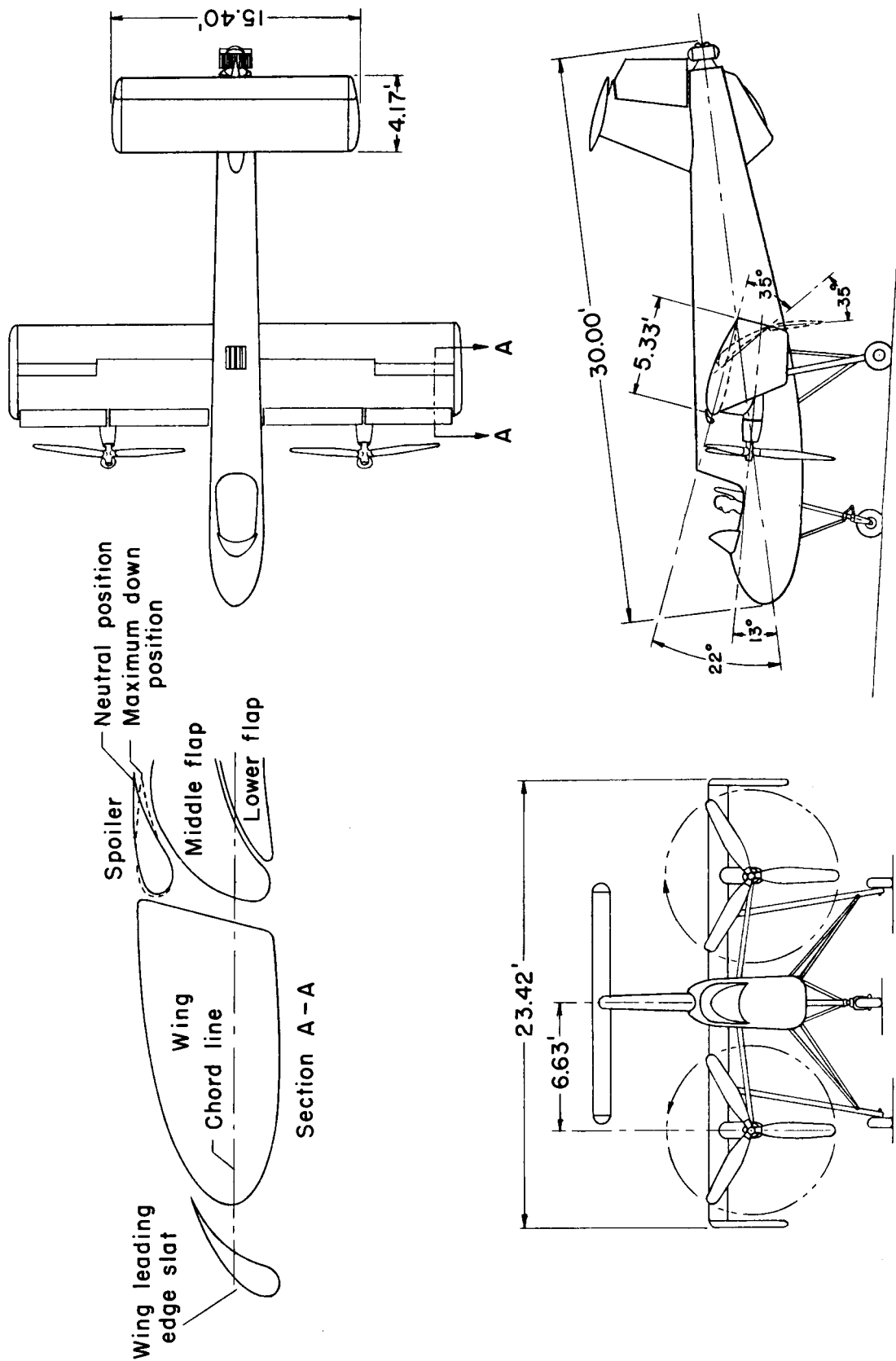


Figure 2.- Three-view drawing of test airplane.

NOTE: DIMENSIONS ARE IN PERCENT FLAPS-UP CHORD

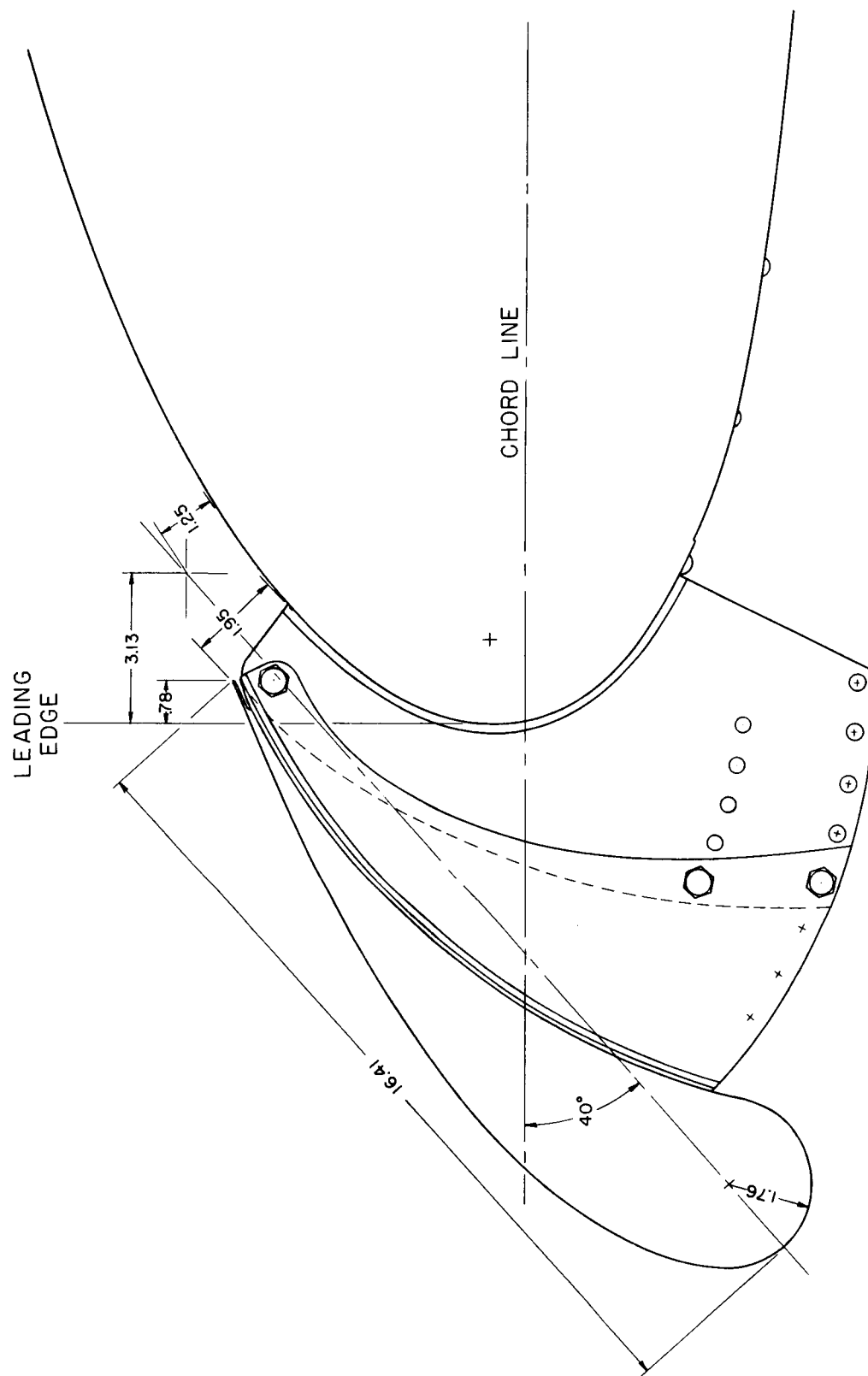
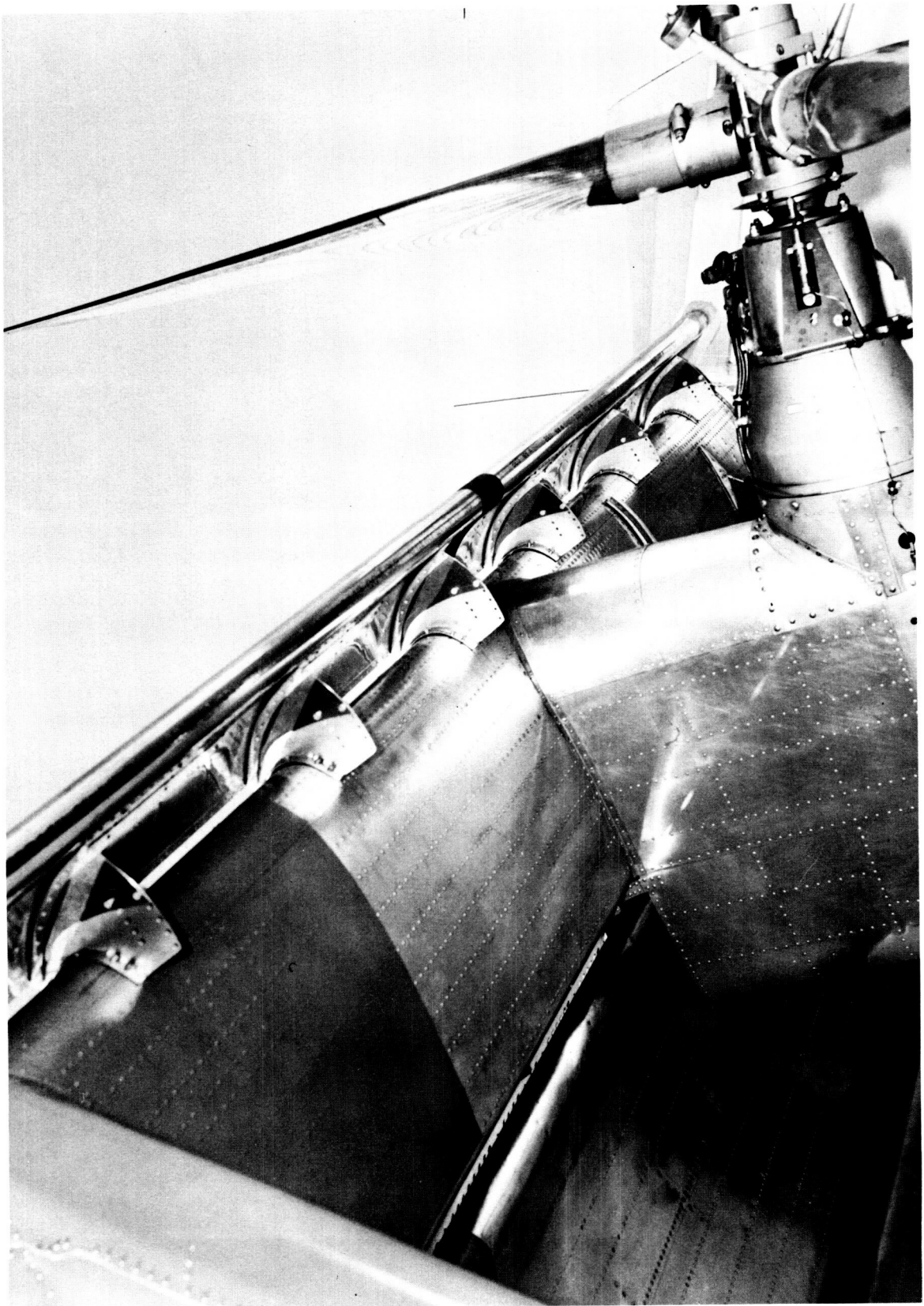


Figure 3.- Wing leading-edge slat layout of test airplane.

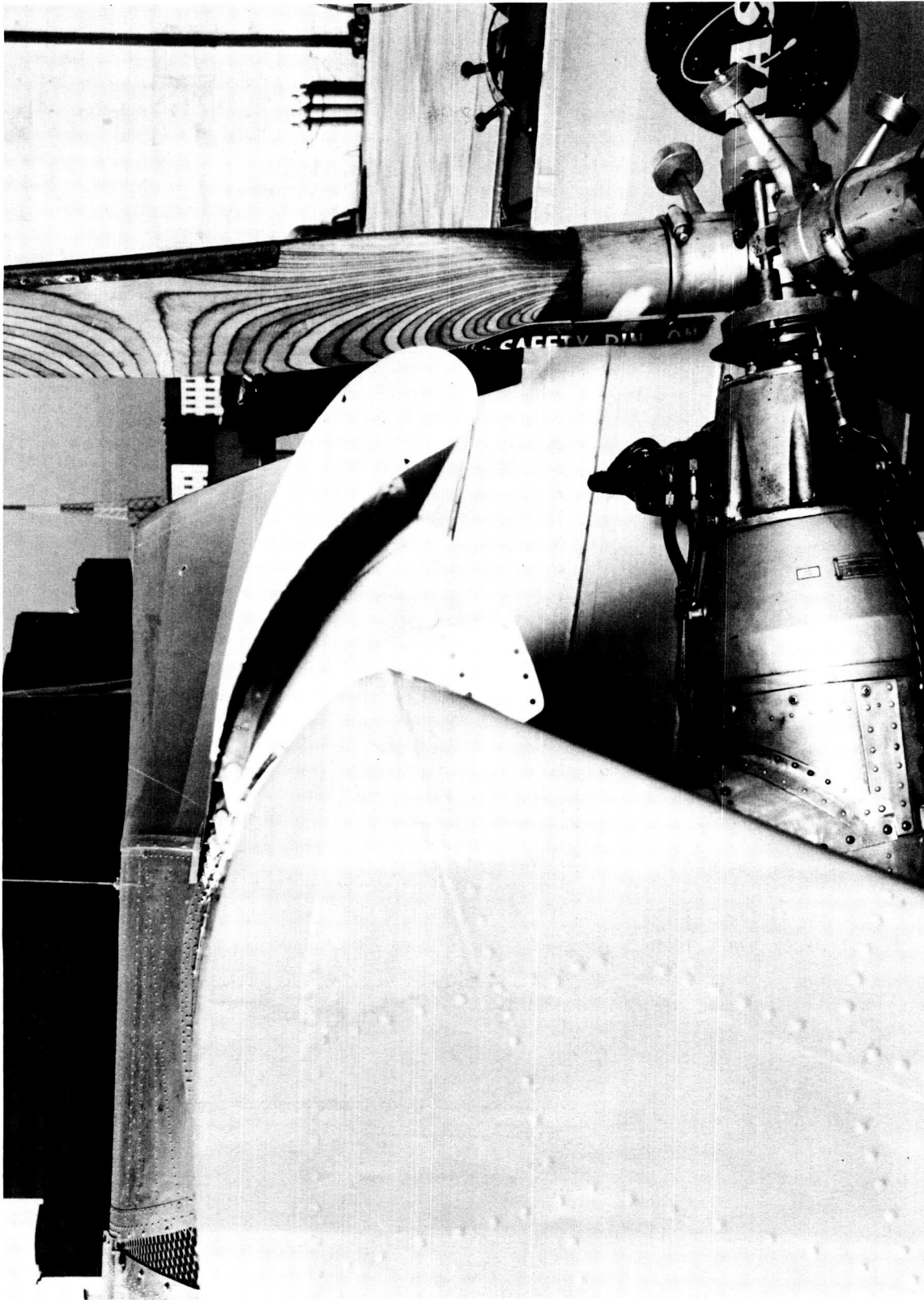




A-29562

(a) Wing attachment.

Figure 4.- Leading-edge slat installation of Ryan VZ-3RY.



A-29561

(b) Slat-wing relationship.

Figure 4.- Concluded.

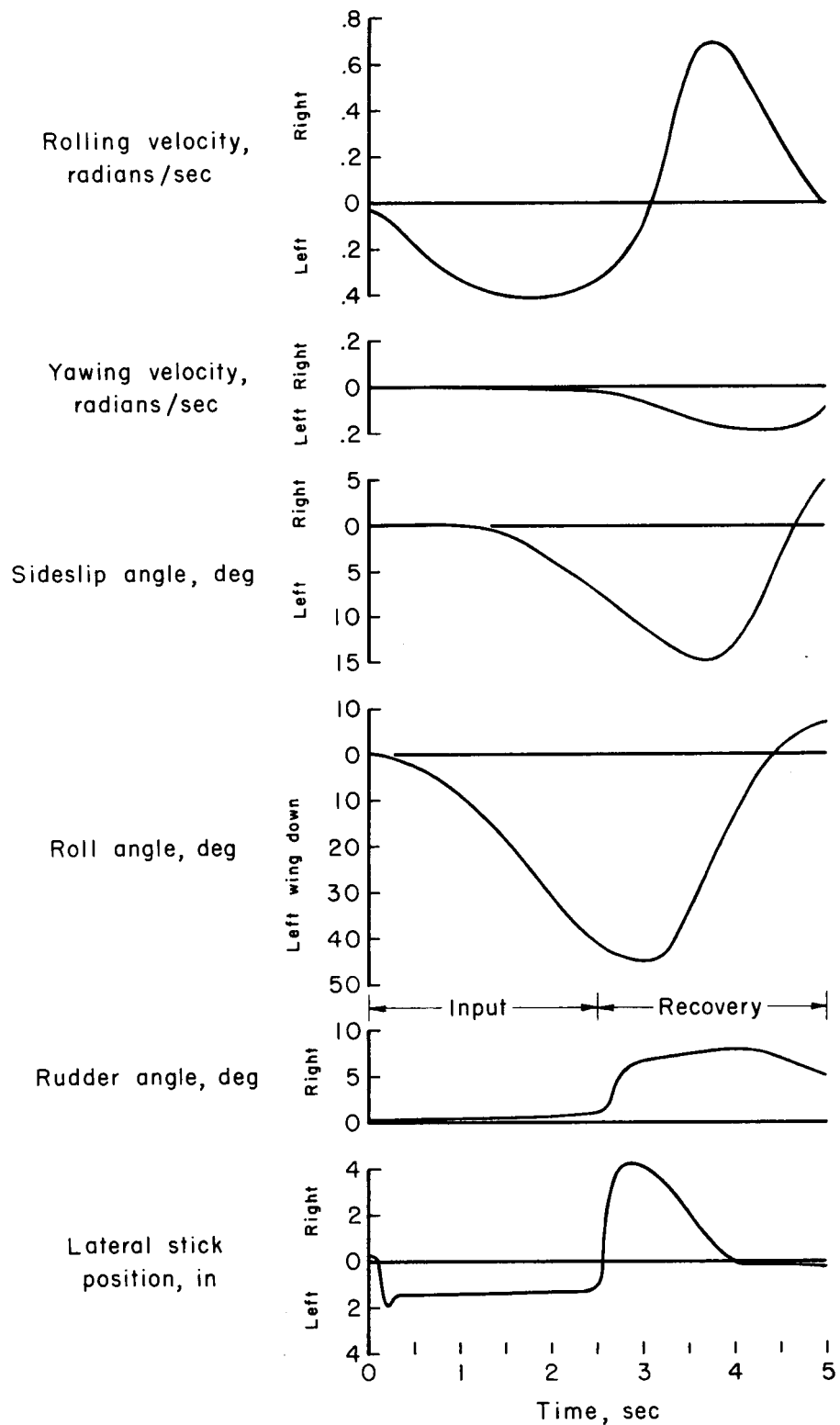


Figure 5.- Time history of the response of a deflected-slipstream test vehicle to a rudder-fixed lateral step disturbance.

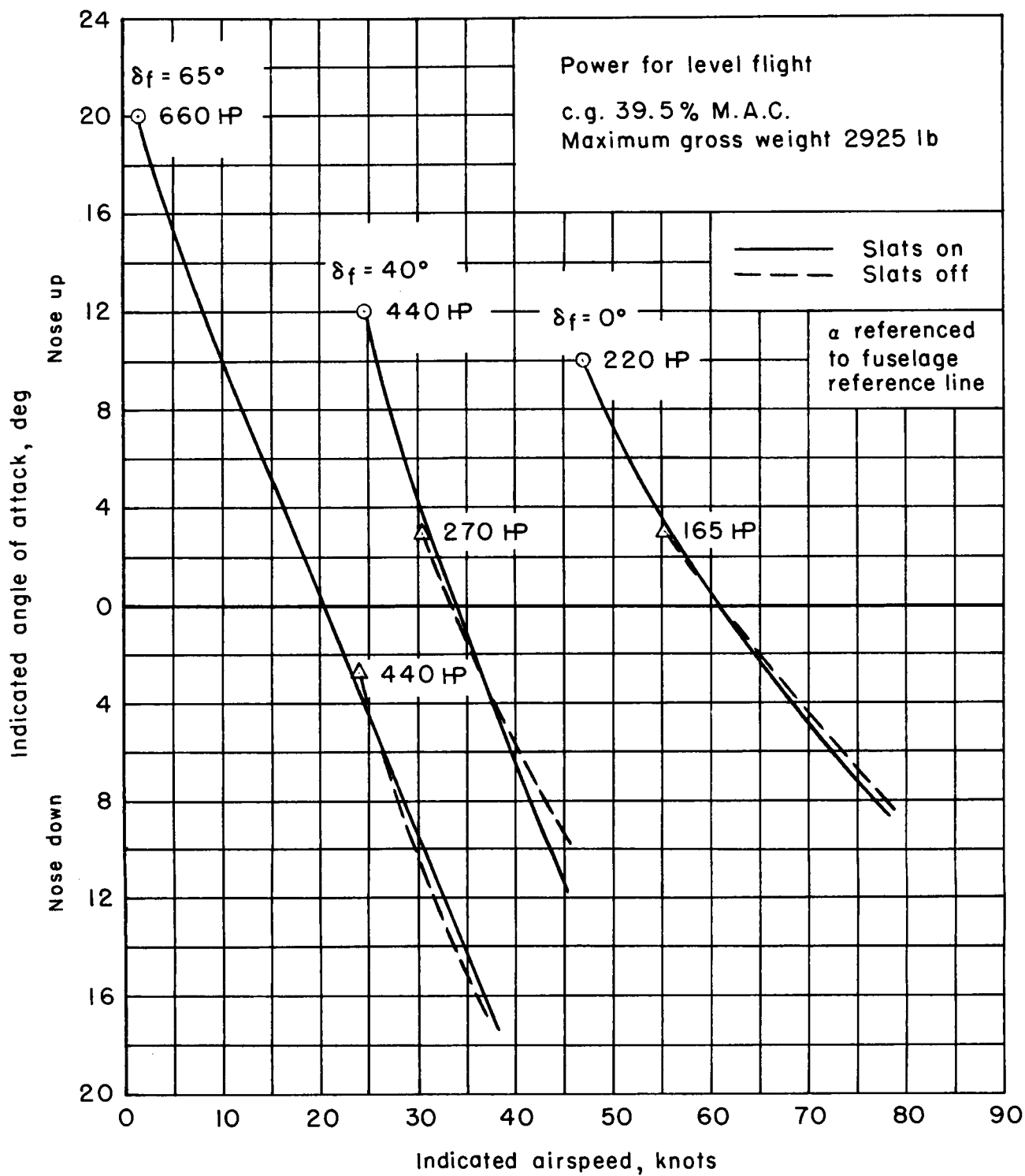


Figure 6.- Angle of attack required for level flight of Ryan VZ-3RY.

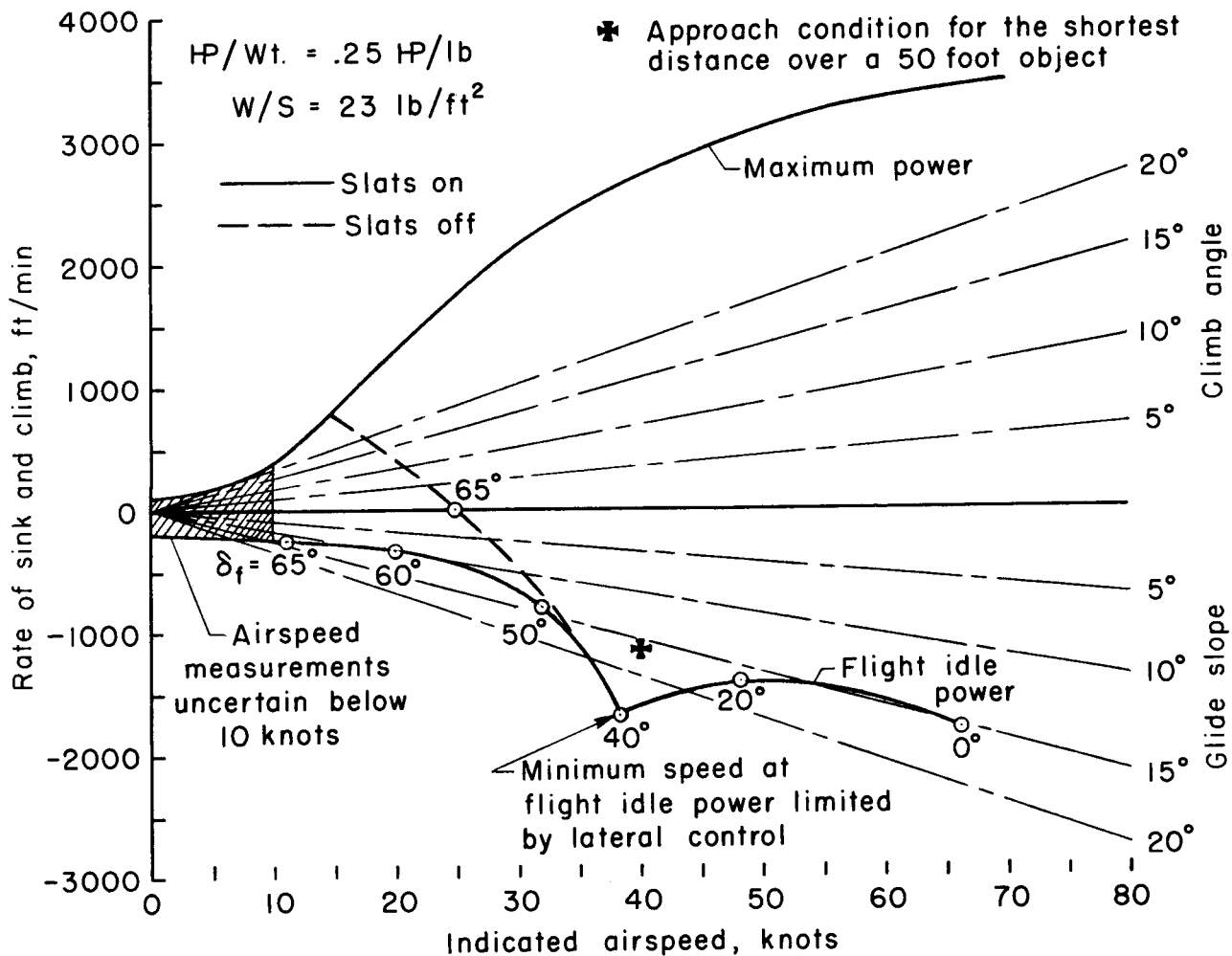


Figure 7.- Flight performance characteristics of deflected-slipstream test vehicle.

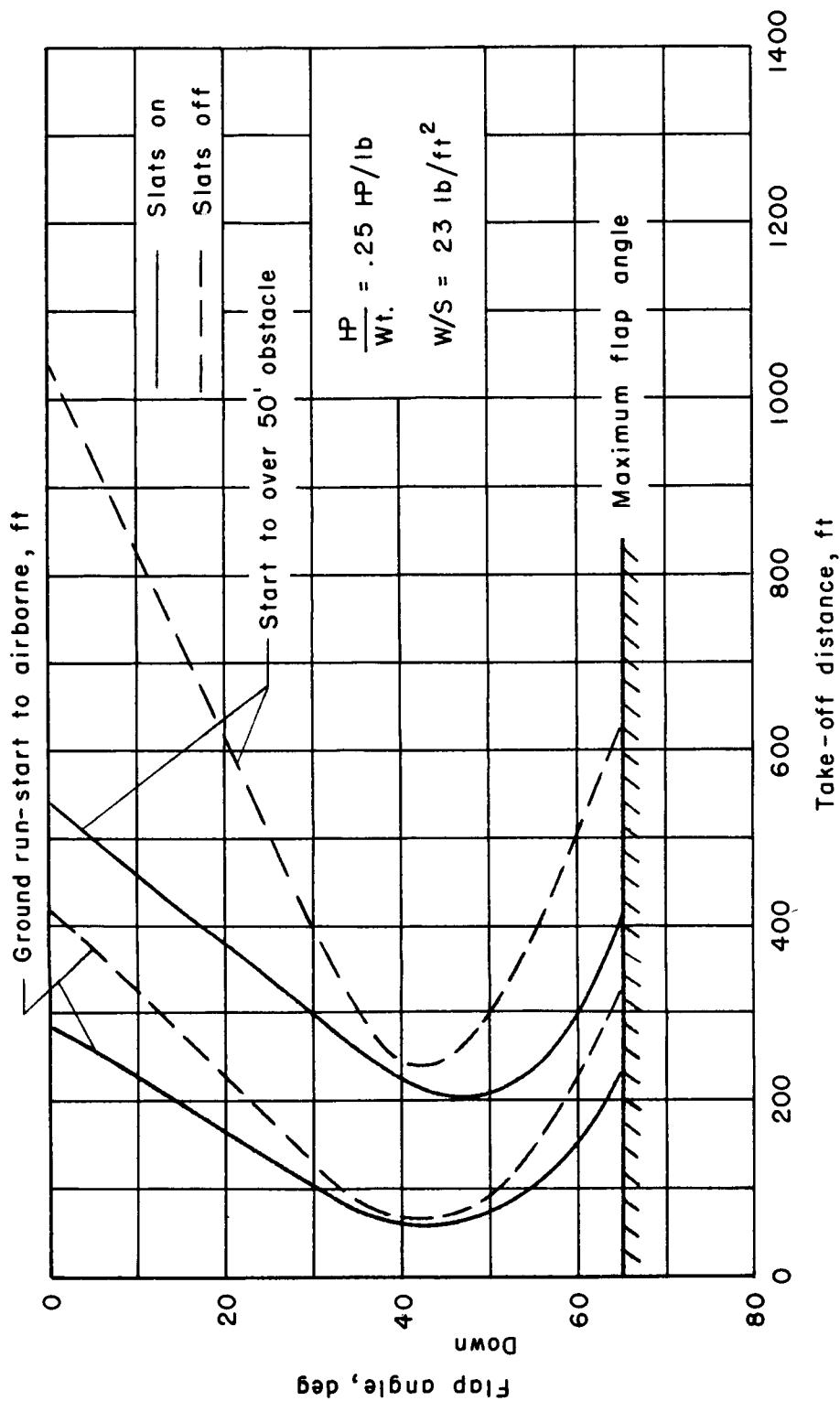


Figure 8.- Take-off characteristics of deflected-slipstream test vehicle;  
surface wind 0 to 9 knots.

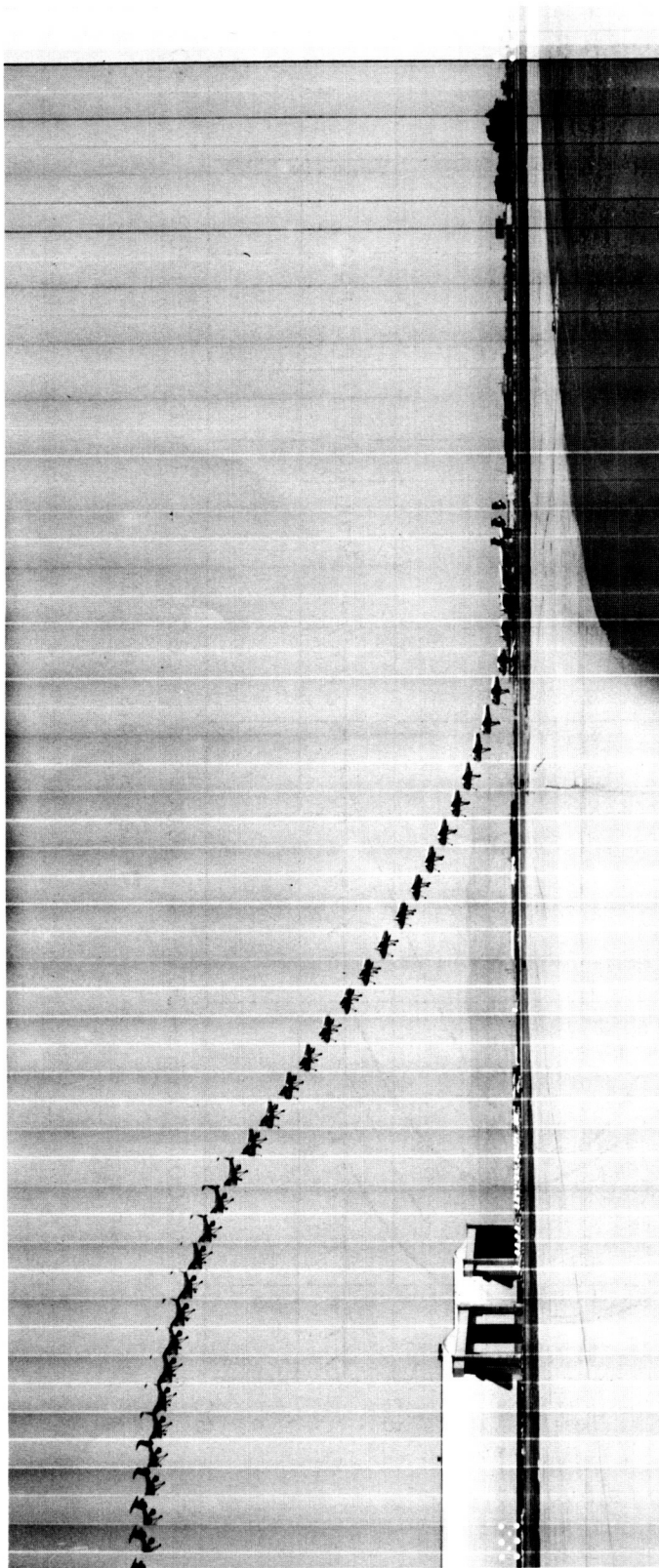


Figure 9.- Typical STOL take-off from a standing start; Ryan VZ-3RY deflected-slipstream test vehicle; wind calm; flap deflection  $40^{\circ}$ .

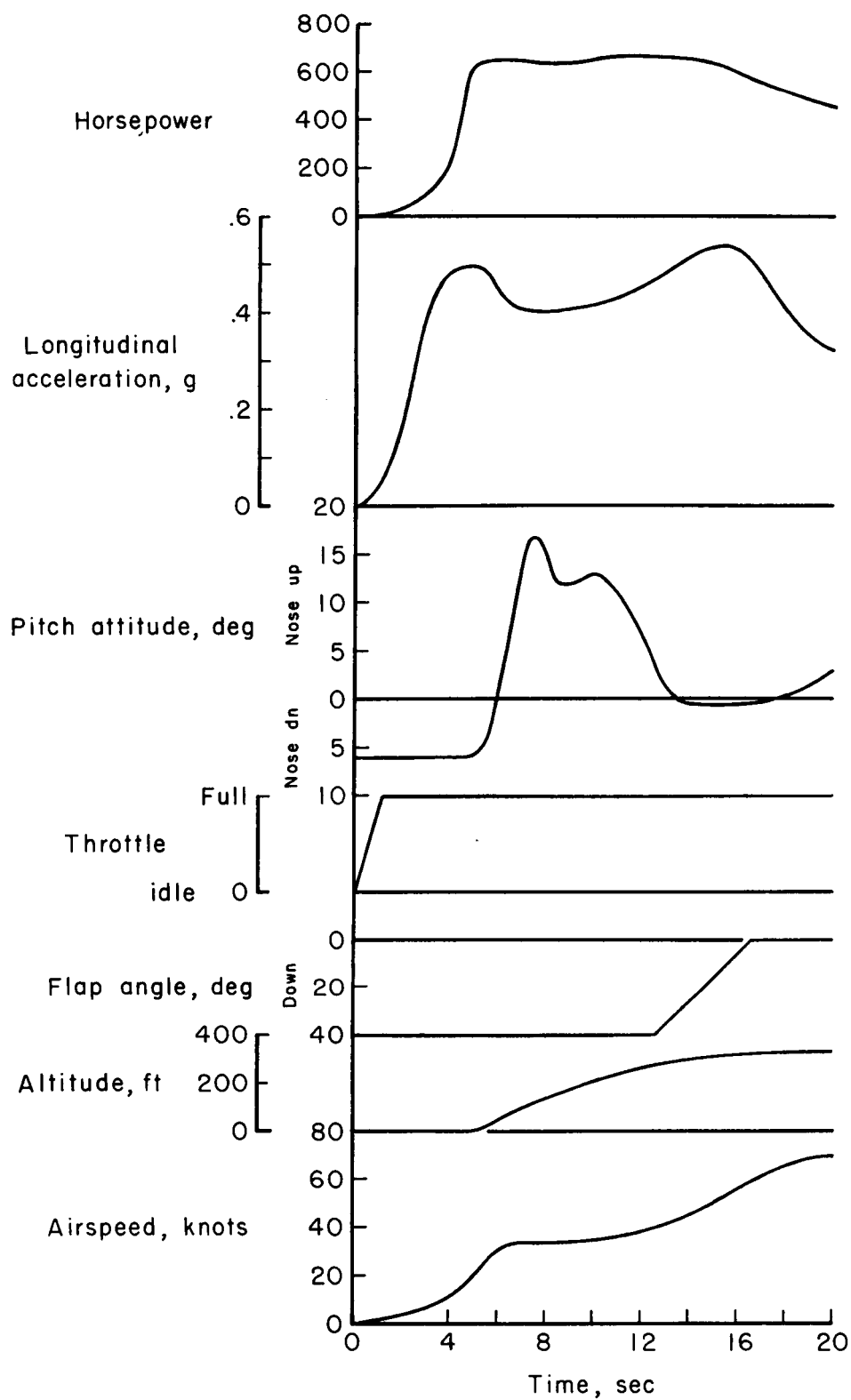


Figure 10.- Time history of a typical short take-off; take-off weight 2,900 lb; surface wind calm.



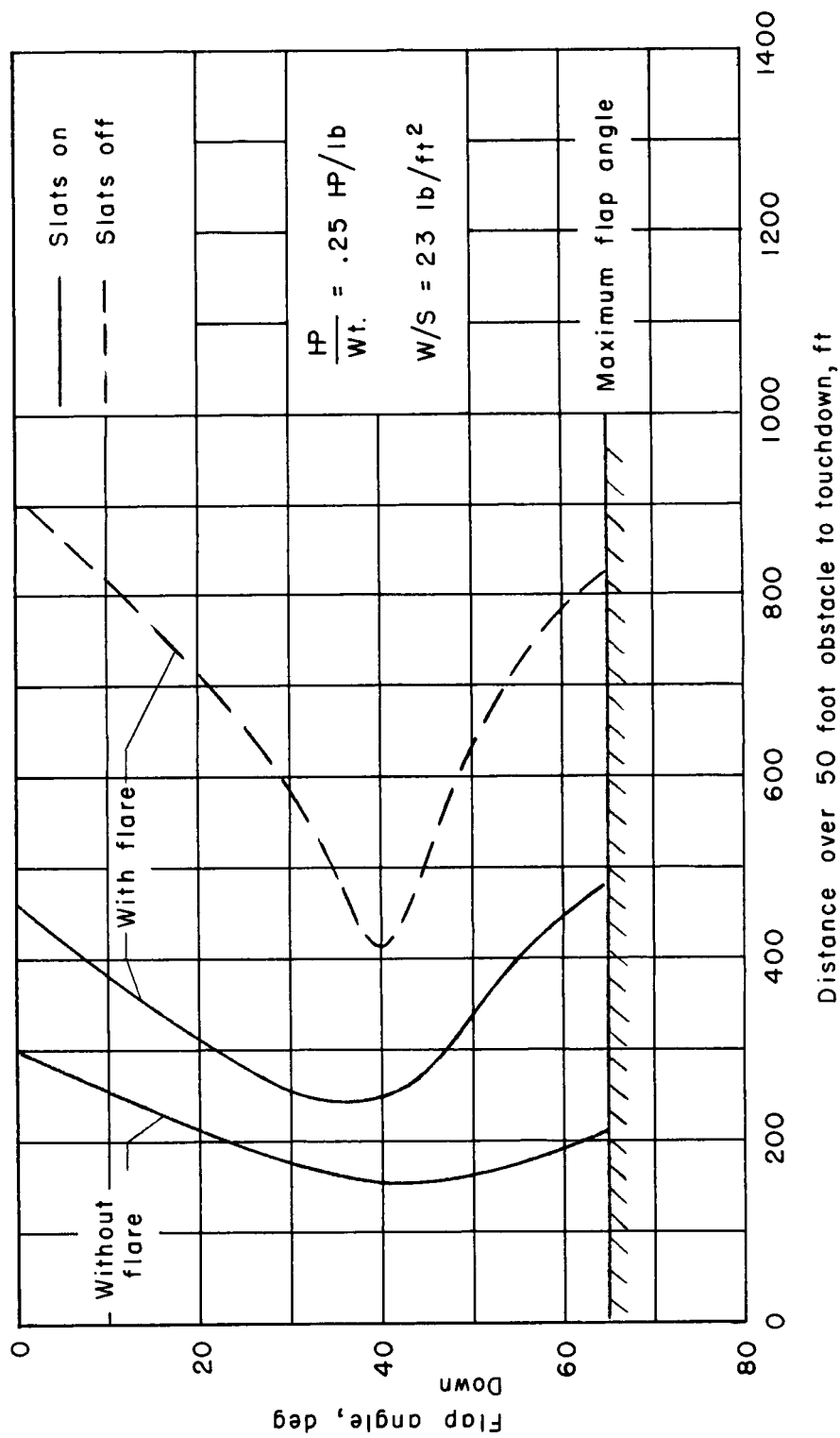


Figure 11.- Landing characteristics of deflected-slipstream test vehicle; surface wind 0 to 9 knots.

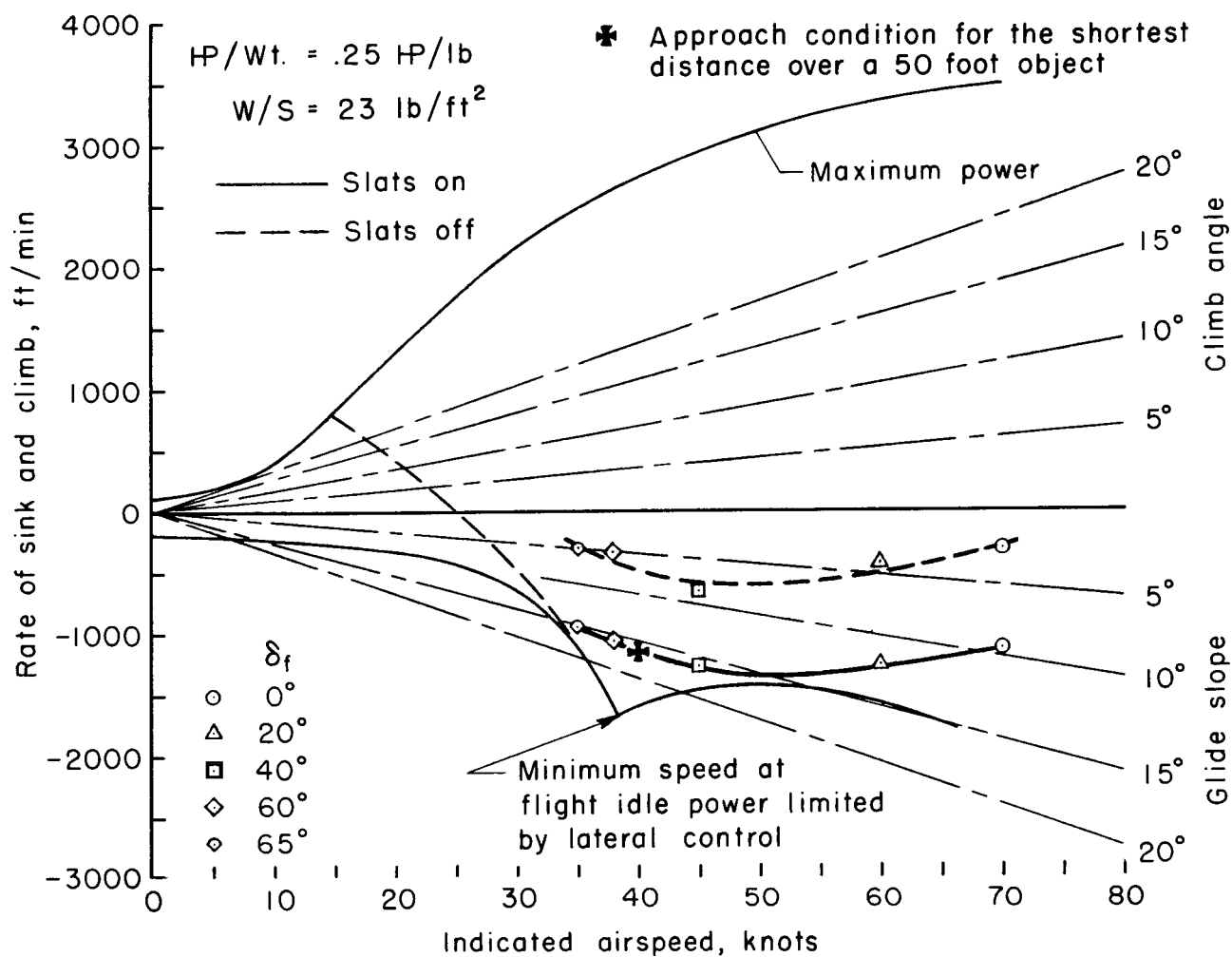
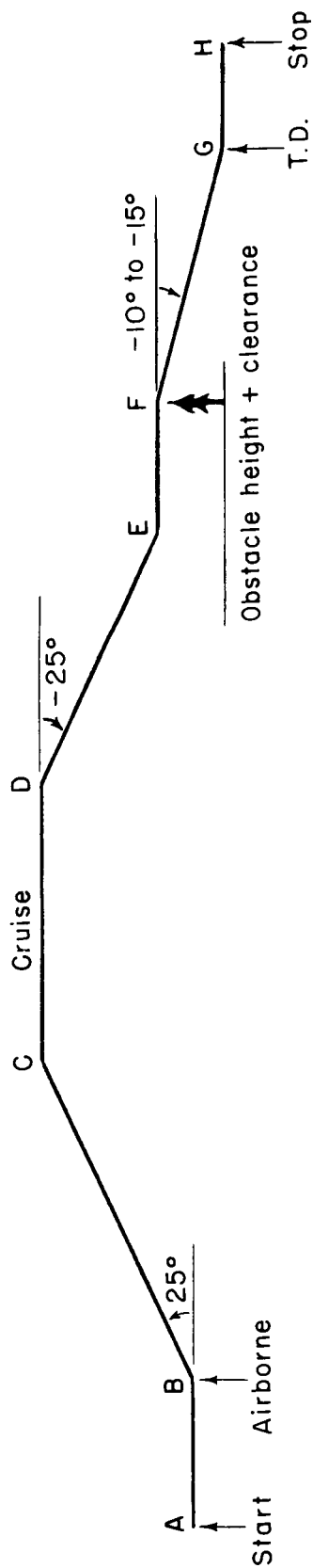
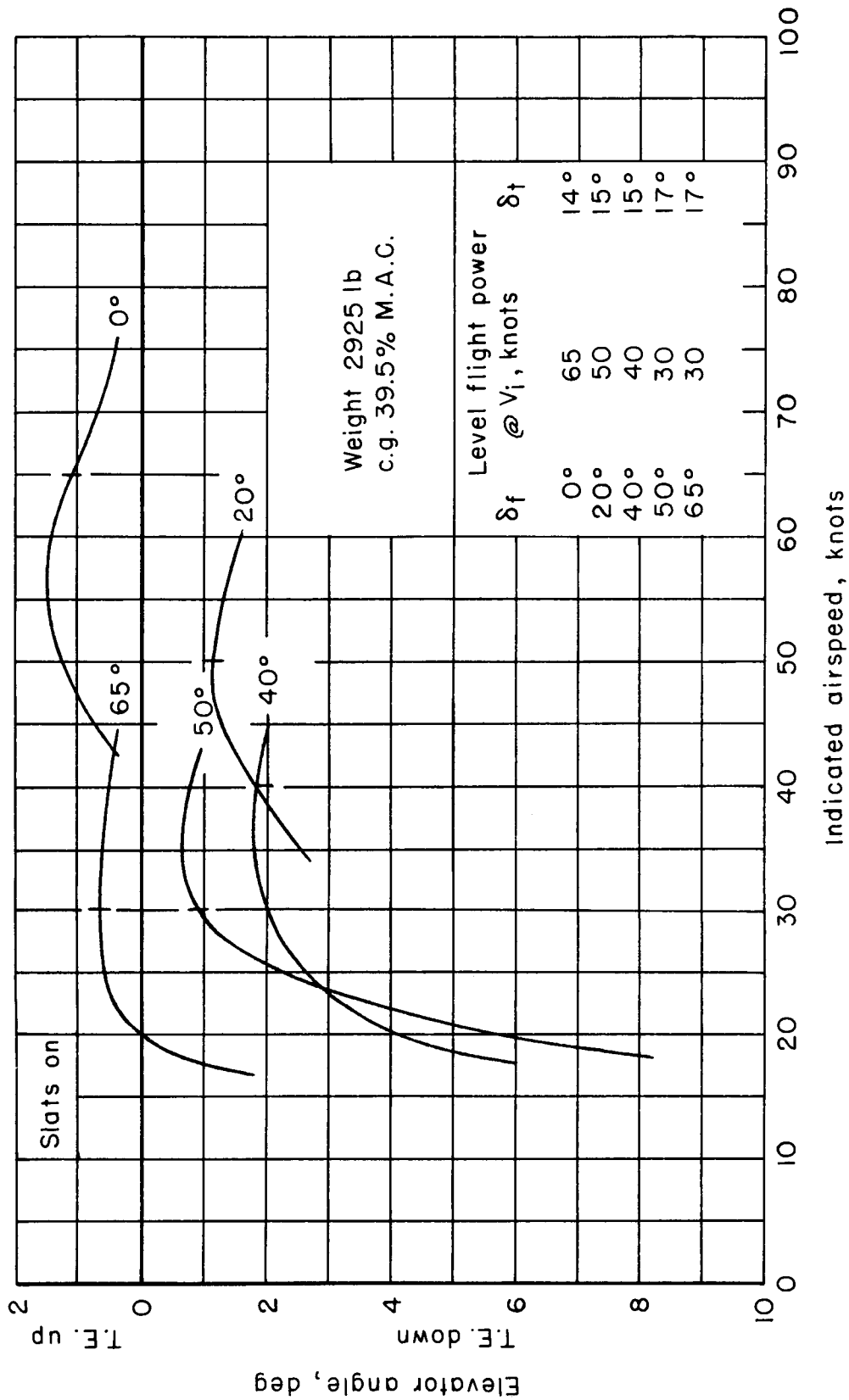


Figure 12.- Descent characteristics of deflected-slipstream test vehicle.



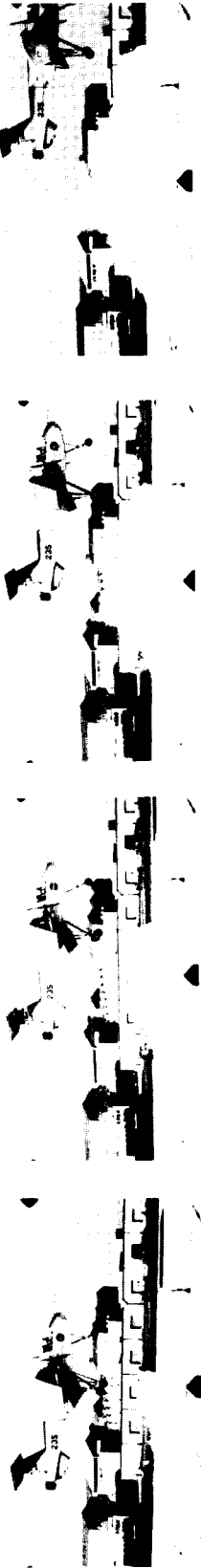
- A to B - Take-off (0.5 to 1.0 g)
- B to C - Climb out to cruise altitude ( $\gamma = +25^\circ$ )
- C to D - Cruise
- D to E - Descent to obstacle height + clearance at  $\gamma = -25^\circ$
- E to F - Level flight destination
- F to G - Final approach to touchdown at  $\gamma = -10^\circ$  to  $-15^\circ$
- G to H - Deceleration to full stop (0.5 to 1.0 g)

Figure 13.- Representative STOL operating profile for a deflected-slipstream aircraft.

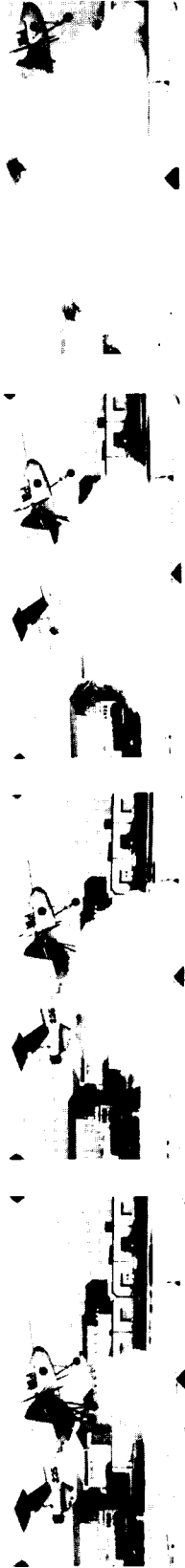


(a) Stick fixed.

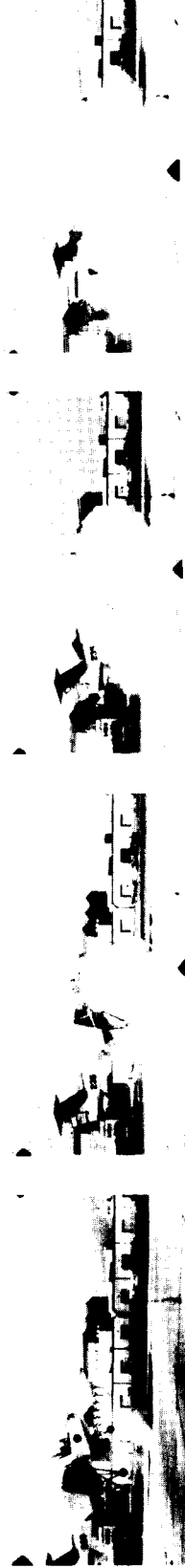
Figure 15.- Static longitudinal stability of Ryan VZ-3RY.



(a) 24 knots; 1.8 propeller diameters above ground; power for level flight; out of ground effect.



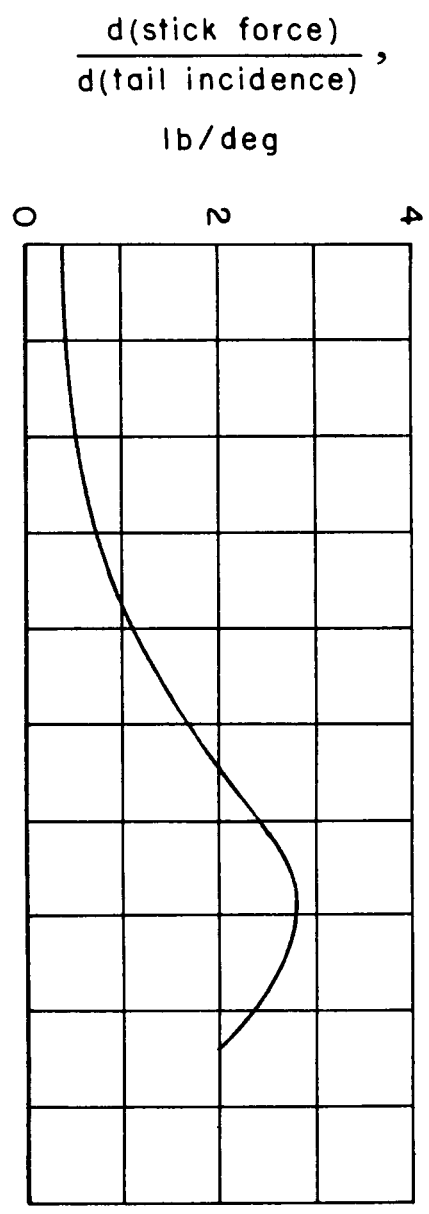
(b) 8 knots; 1.8 propeller diameters above ground; maximum power; out of ground effect.



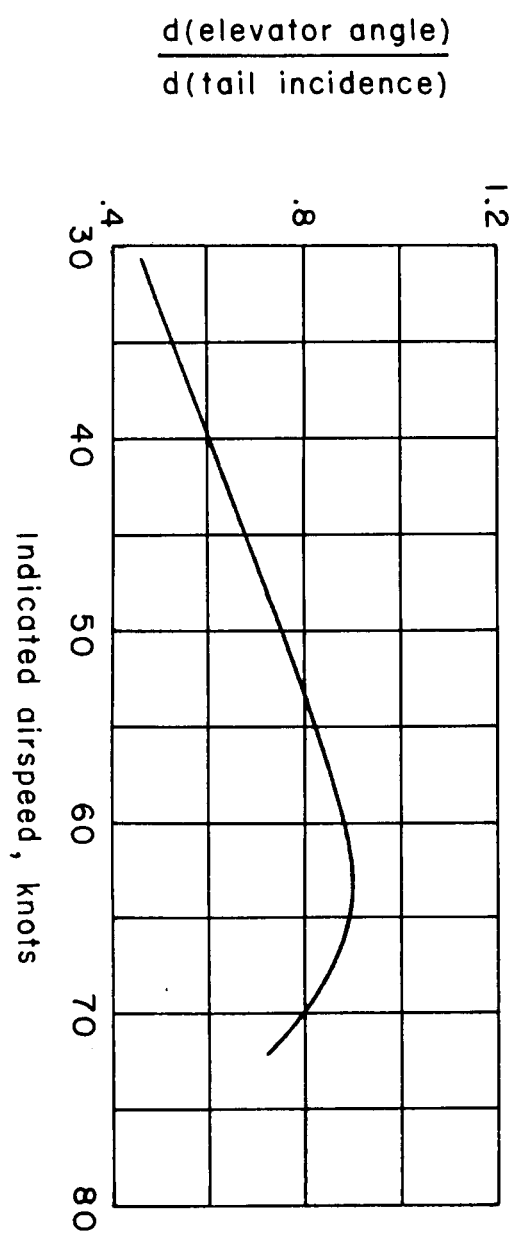
A-30240

(c) 8 knots; 1 propeller diameter above ground; maximum power; in ground effect.

Figure 14.- Pictorial indication of slipstream recirculation of Ryan VZ-3RY deflected-slipstream test vehicle with flap deflected  $65^\circ$ ; surface wind calm.

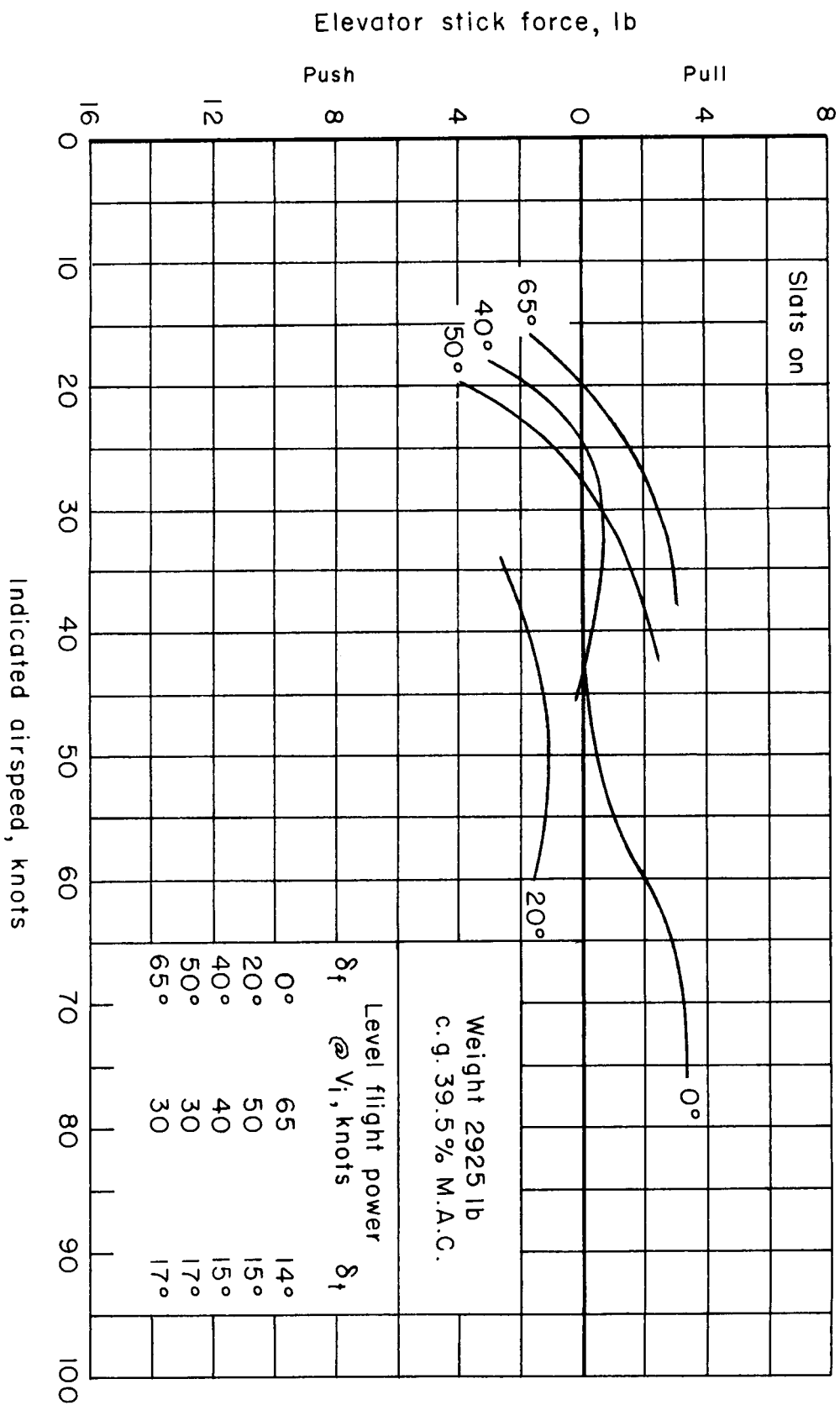


c.g. 39.5 % M.A.C.  
Maximum gross weight 2925 lb

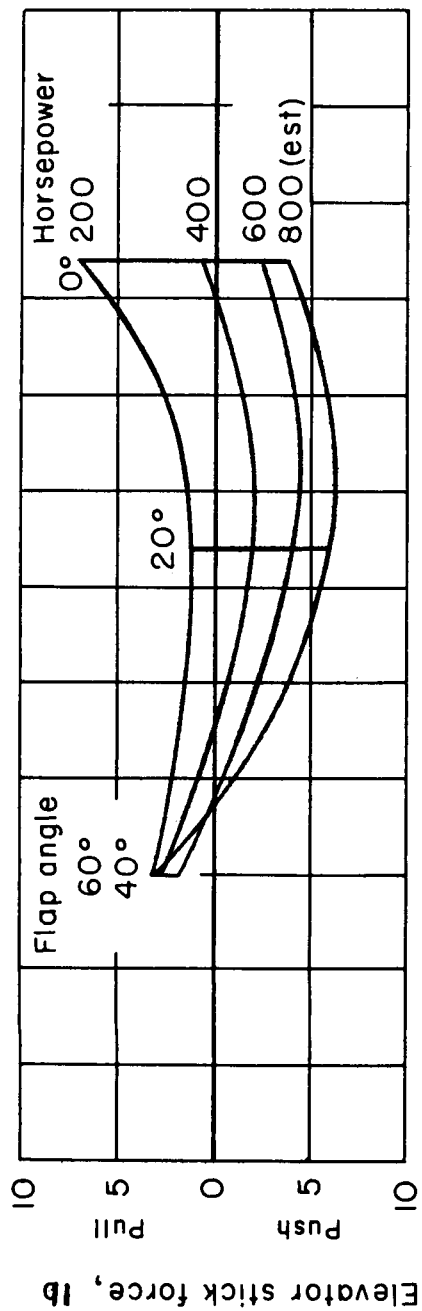


(a) Horizontal-tail effectiveness.

Figure 16.-- Longitudinal trim characteristics of Ryan VZ-3RY.

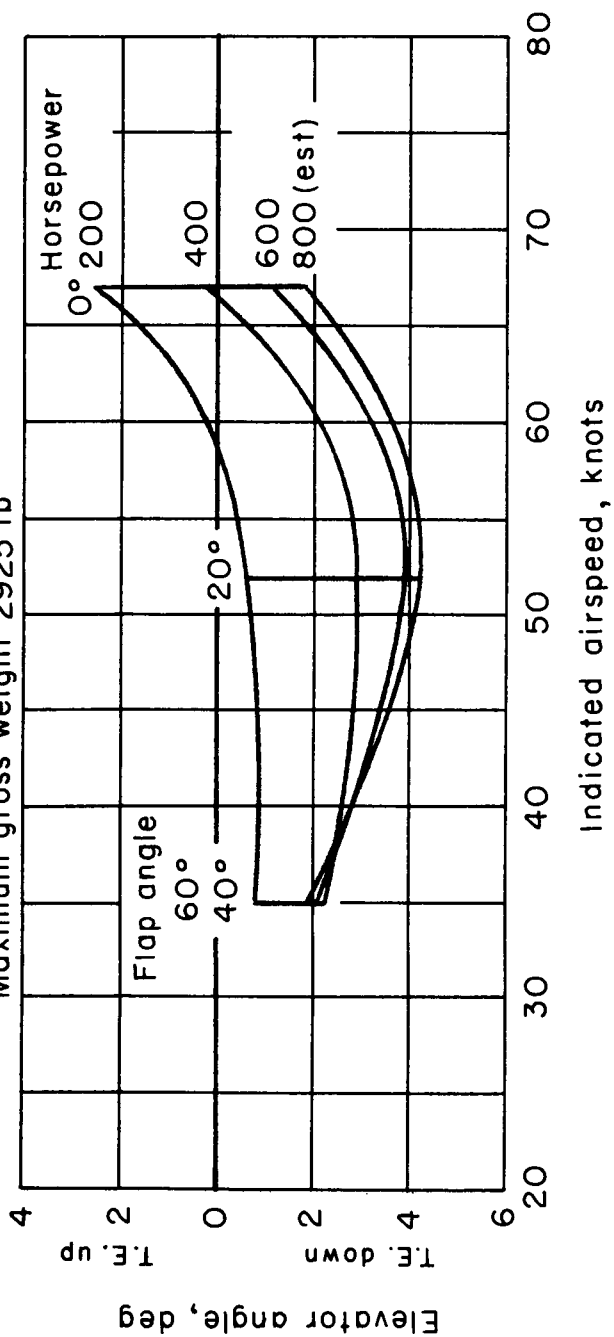


(b) Stick free.  
Figure 15.- Concluded.



c.g. 39.5% M.A.C.

Maximum gross weight 2925 lb



(b) Trim change with flap and horsepower.

Figure 16.- Concluded.



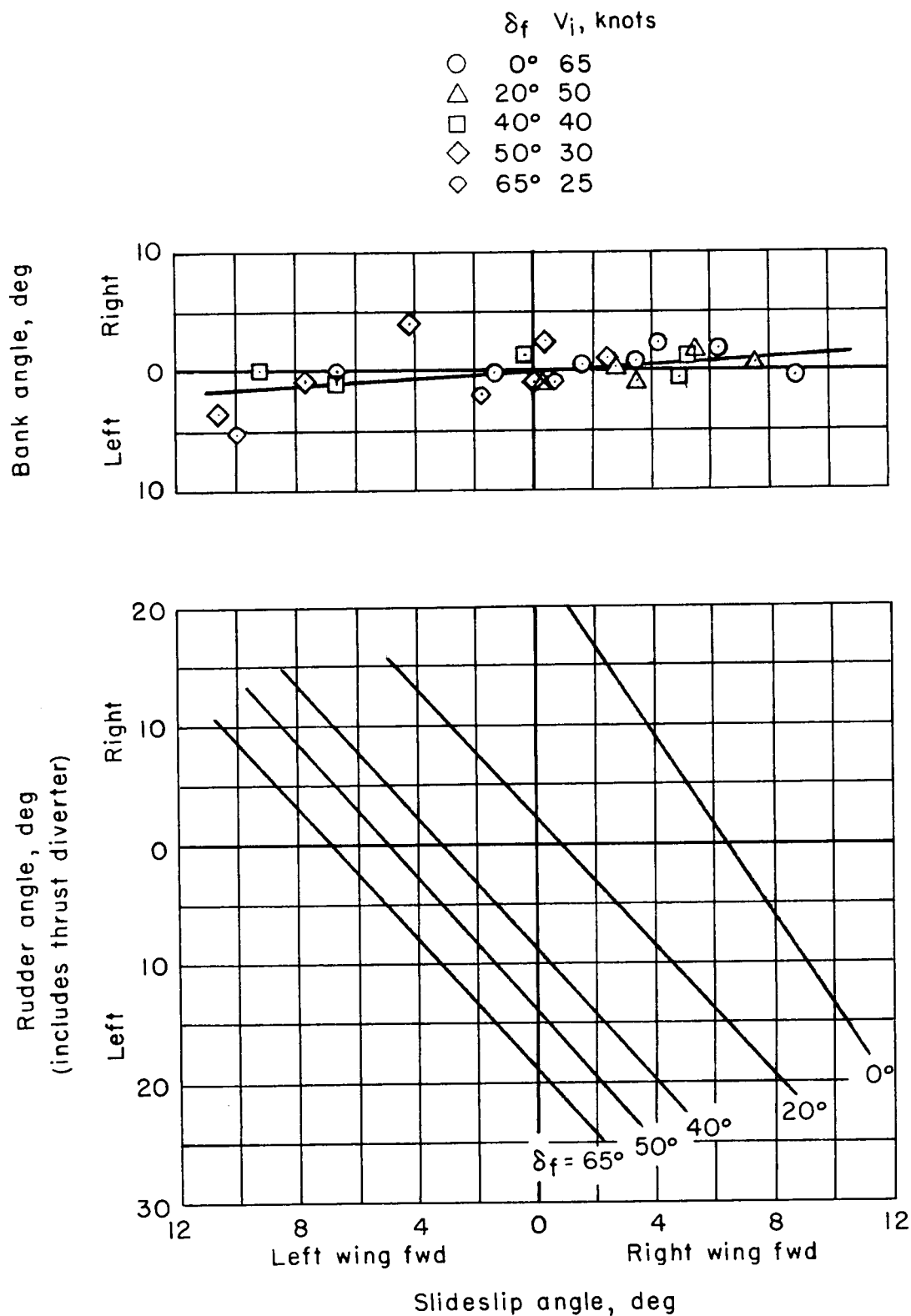


Figure 17.- Directional stability characteristics of Ryan VZ-3RY.

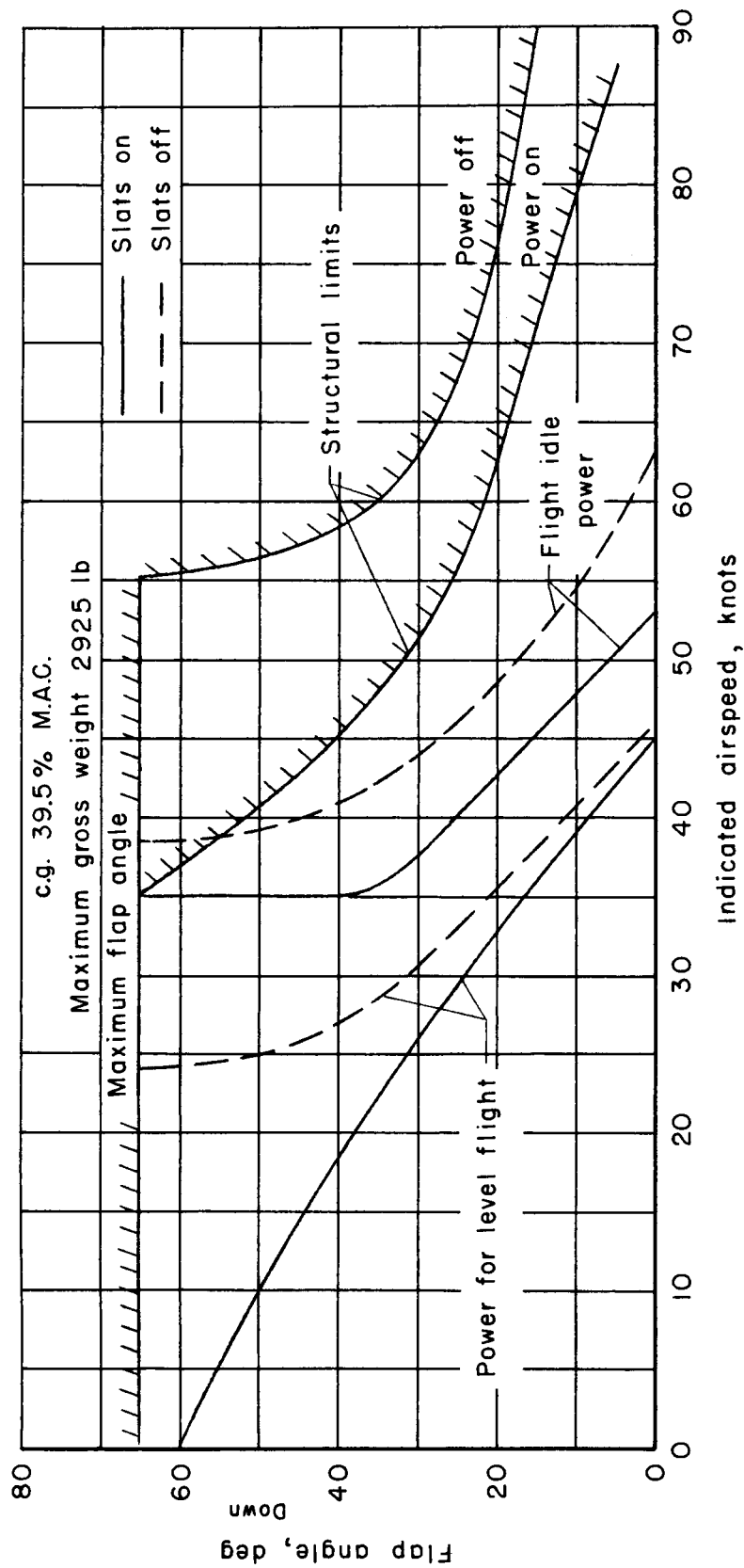


Figure 18.- Flight operating boundaries of Ryan VZ-3RY.